ALUMINUM OXIDE PARTICLES PRODUCED BY SOLID ROCKET MOTORS

R. Dawbarn
ARO, Inc.
A Sverdrup Corporation Company
Arnold Air Force Station, Tennessee

The candidate propellant for the Shuttle solid rocket motors contains approximately 16 percent aluminum powder. In this percentage range the aluminum can be considered as a significant portion of the fuel. However, it serves a dual purpose in that it also tends to stabilize the burning process. It has long been recognized that combustion instabilities in solid rocket motors can be alleviated by adding powdered metals to the fuel mix. There is therefore a considerable source of literature and data concerning metal oxide particles produced by solid propellant rocket motors. However, before embracing these data and applying them to environmental and contamination concerns posed by Shuttle operations one should be fully aware of the prime interest which prompted these previous studies.

1.0 DAMPING COMBUSTION INSTABILITIES

The combustion rate of solid propellants is pressure sensitive. Therefore, acoustic waves which may be generated within the combustion cavity can cause accelerated burning at the anti-nodes. If this accelerated burning feeds pressure pulses back into the acoustic field in a resonant mode then the resulting undamped system can lead to a violent failure of the rocket motor. It has been found that these instabilities can be damped by the inclusion of the metal oxide particles in the acoustic field in the combustion cavity. Figure 1 presents the curves showing attenuation $\alpha D/cm$ versus particle size for three frequencies as derived from the theory of Temkin and Dobbins and calculated by

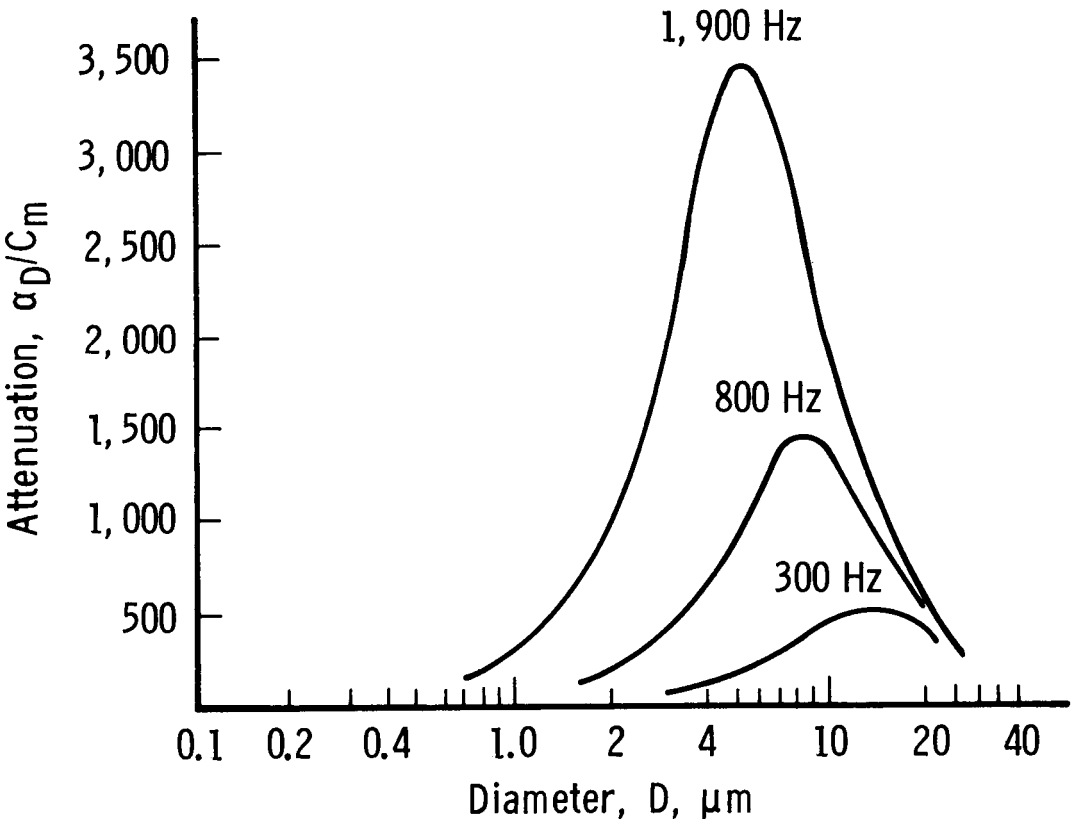

Fig. 1 Attenuation α_D/C_m versus Diameter (Ref. 1)
(Calculated for C_m = 0.02)

Dehority.[1] As can be seen, the range of particle size of interest is from 0.5 μm to 50 μm, with the bulk of the attenuation for low frequencies being produced by particles in the 2-20 μm range. However, while these larger particles are beneficial inside the combustion cavity, they are detrimental to rocket performance (specific impulse) as they are ejected along with the gases through the nozzle. With a requirement for a sufficient number of large dampers to maintain combustion stability, yet a need to limit the number of particles in the flowfield to an absolute minimum, the processes involved in the formation of the oxide particles are of great interest. Many experiments have been conducted and attempts made to collect samples of these oxide particles to determine their number and size distribution. Since the particle sizes of interest for damping and specific impulse loss have been from 2-50 μm, the majority of the collection techniques as well as the counting and sizing methods have been oriented toward this size range. Thus in many cases the submicron particles have been ignored.

1.1 Mean Diameters

In some instances it is convenient to refer to a particular size distribution of particles in terms of a mean particle diameter. The most commonly understood mean diameter is the linear mean, i.e.,

$$\bar{d}_{10} = \frac{\Sigma d dn}{\Sigma\, dn} \tag{1}$$

However, other mean diameters are also calculated and used depending on the particular field of application. In general the mean diameter can be of the form

---

[1] Dehority, G. L., "A Parametric Study of Particulate Damping Based on the Model of Temkin and Dobbins," NWC TP 5002, Sept. 1970.

$$\bar{d}_{qp}^{(q-p)} = \frac{\int_{d_o}^{d_{max}} d^q \frac{dn}{dx}\, dx}{\int_{d_o}^{d_{max}} d^p \frac{dn}{dx}\, dx} \qquad (2)$$

where p can take integral values from 0 to 3 and q from 1 to 4. Each combination of p and q places a specific emphasis on a particular size range within the distribution. For example, the linear mean $\bar{d}_{10}$ heavily emphasizes a large number of small particles whereas a $\bar{d}_{43}$ mean, minimizes the contribution of the smaller particles. Since the larger particles are of prime concern in combustion stability and two-phase flow losses the $\bar{d}_{43}$ mean diameter is usually reported; i.e.,

$$\bar{d}_{43} = \frac{\Sigma d^4\, dn}{\Sigma d^3\, dn} \qquad (3)$$

This method of summarizing the experimental data has led to a misconception of the total range of particle sizes produced by solid rocket motors and has fostered a false impression that there is a general consistency in the data collected from the various test programs. Figure 2 presents raw data in the form of bar graphs of particle size distributions obtained from Al_2O_3 samples taken from Titan IIIc firings. The samples were analyzed using the same methods but were collected using different techniques. As can be seen, the size distributions are radically different insofar as the number of small particles reported, whereas the calculated mean particle size from these two data sets are d_{43} = 11.4 μm and 12.6 μm. The mass weighted mean which would seem in reasonably good agreement is adequate for combustion studies. However, the data are inconsistent when one is concerned with the possible effects of contamination by smaller particles.

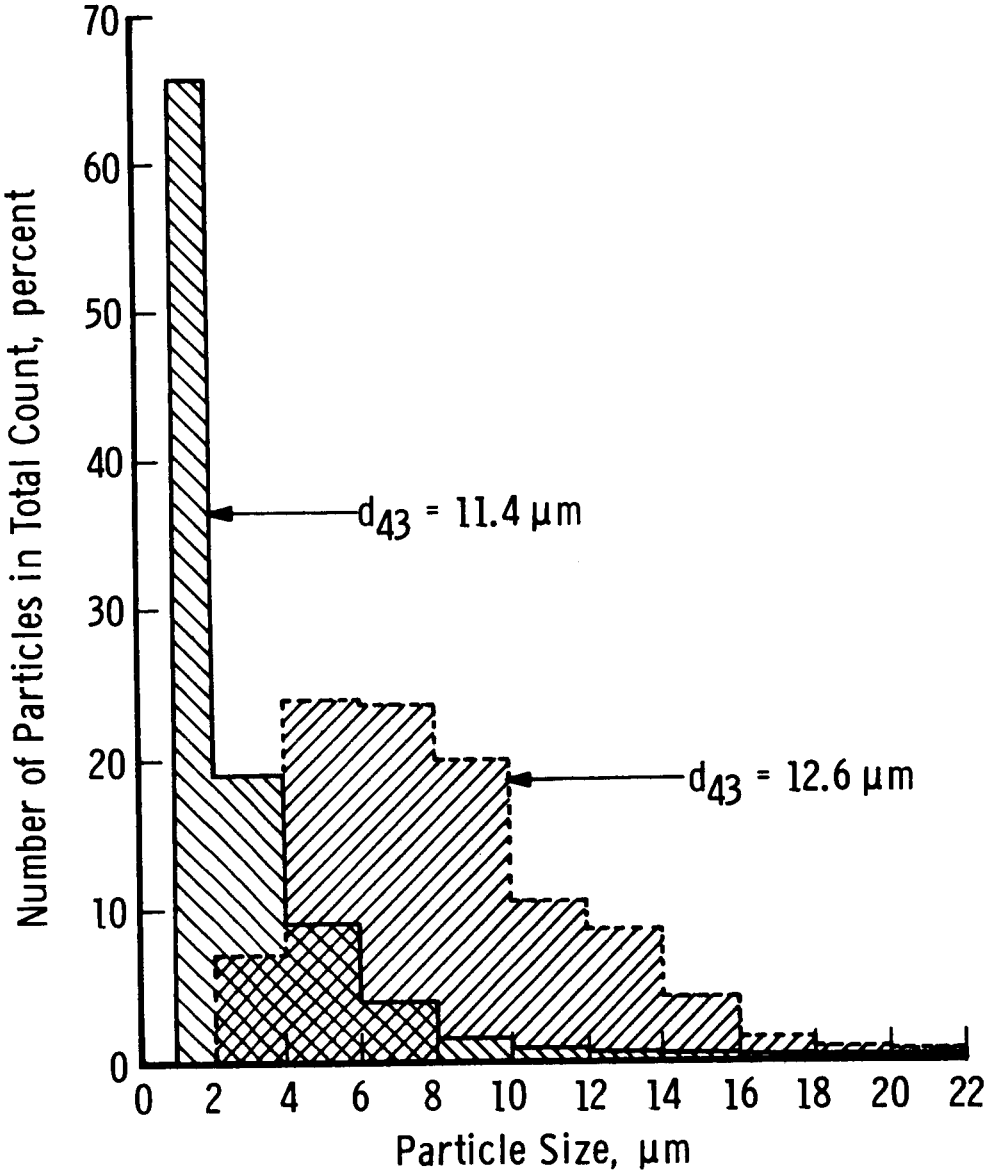

Fig. 2 Histogram from Titan IIIc Samples

1.3 Particle Size Distribution Functions

There are several ways of presenting particle size distributions. In addition to the histogram, there is a variety of distribution functions, and again one finds the format chosen, determined by the eventual use of the experimental data. In order to compare data from various sources, particle size information presented in this paper has been fitted to a distribution function.

1.3.1 Fitting Data to Distribution Function

There are several mathematical functions which have been used to provide a representation of particle size distributions. In many ways they are all variants of the expression

$$\frac{dN}{dD} = aD^p \, e^{-bD^n} \tag{4}$$

In some cases an attempt is made to relate one or more of the constants (a,p,b,n) to some physical parameter of the particle formation process. Nukiyama and Tanasawa[2] obtained extensive data of drop sizes in sprays formed by air atomization and from these data defined p = 2 and n $\approx$ 1 for these sprays with b some undetermined function of the physical characteristics of the liquid, nozzle design and the relative velocity of the liquid and air. Similarly Worster et al.[3] using available data on Al_2O_3 particle sizes defined p = 3 and proposed a functional relationship between the constants a and b and the throat diameter of the rocket motor which produced the particles. Rosen et al.[4] used a semi-empirical

---

[2] Nukijama S. and Tanasawa, Y., "An Experiment on the Atomization of Liquid by Means of an Air Stream (1st report)," Trans. S.M.E. Japan, Vol. 4, No. 14 (Feb. 1938).

[3] Worster, B. W. and Kadamiya, R. H., "Rocket Exhaust Aluminum Oxide Particle Properties," ARl RR-30 (Aug. 1973).

[4] Rosin, P. and Rammler, E., "The Laws Governing the Fineness of Powdered Coal," Journal of the Inst. of Fuel, Vol. 7, 1933.

technique to derive a functional relationship between the constants to fit the equation to data obtained from grinding coal dust. In this case $p = n-4$ and $a = 6bn/\pi$, with b and n determined empirically.

It would appear that the possibility of defining the constants in terms of such fundamental physical properties as viscosity, surface tension, density, etc. of the particles and the force fields in which they are formed is very remote. However, the apparent universality of this function in its ability to fit the size distribution of particles formed by a variety of processes can be used to advantage in comparing data such as those obtained in collections of Al_2O_3 from rocket exhausts. It is particularly useful in that it predicts a finite number of small particles and defines a specific particle size where the distribution peaks. In many experimentally observed particle collections this peaking of the data is noted (Figs. 4 and 9). However, in some samples which are collected, due to the collection technique or the method of analysis, the data are truncated and the peak is missed. In the curves presented in this paper the data were used to obtain the best fitting distribution function and the resulting peaking of the distribution function is thus in some cases an "extrapolation" ofthe distribution below the observed particle size. All distributions have been normalized to this maximum peak or mode for ease of comparison.

The following method was used to choose the appropriate values of the constants a, b, n and p. The distribution function can be rewritten as

$$\log\left(\frac{1}{D^p}\frac{dN}{dD}\right) = \log a - b\,D^n \log e \qquad (5)$$

Thus, the data were plotted as $\log\left(\frac{1}{D^p}\frac{dN}{dD}\right)$ against D^n for various values of n and p. The values of n and p were adjusted for the best straight line fit. For the majority of the data examined, values of $n = .3$ and

p = 2 were satisfactory. The total range of values was n = (.3 → 1.0) and p = (1 → 3). From these data fits, values of a and b can be calculated from the slope and intercept. In order to obtain some uniformity in plotting the distribution functions they were normalized at their mode. The mode was determined by setting

$$\frac{d}{dD}\left(\frac{dN}{dD}\right) = 0 \tag{6}$$

and thus $D = n\sqrt{\frac{P}{bn}}$ for the maximum value of $\left(\frac{dN}{dD}\right)$.

2.0 COMPARISON OF Al_2O_3 PARTICLE SIZE DATA

Data obtained from many rocket motor firings, using a variety of collection techniques have been combined to support the hypothesis that the mean particle size produced by solid rocket motors is a function of the throat diameter of the rocket.

Samples of data used to obtain this correlation along with the empirical distribution function are presented in Figs. 3 and 4. As can be seen, the correlation does a fair job of accommodating the data, especially when one considers the orders of magnitude difference in the size rocket motors presented in these two examples. Confidence that such a correlation does indeed exist is greatly shaken, however, when one compares data presented in Fig. 5. These data all represent particle size distributions of particles from Titan III-C rocket motors, taken using different collection techniques. As can be quite readily seen, the data indicate a wide variety of size distribution functions. It is also of interest to note that the size distributions (curves 3 and 4) as determined by two separate laboratories analyzing the same sample are not in agreement. Thus it would appear that even with the same samples and using similar sizing techniques the results, while close, are not

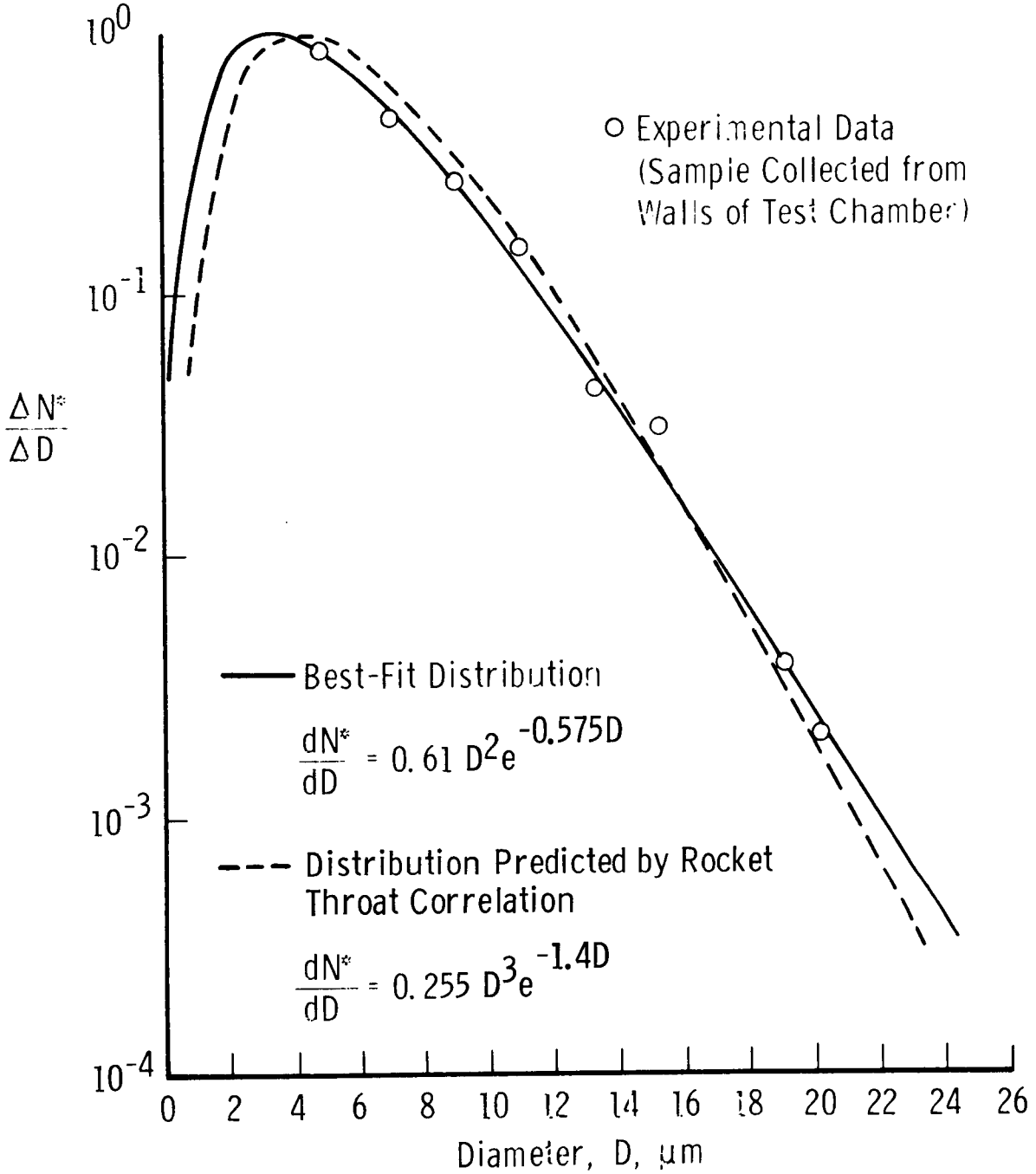

Fig. 3 Small Research Motor (0.85-in. Throat)

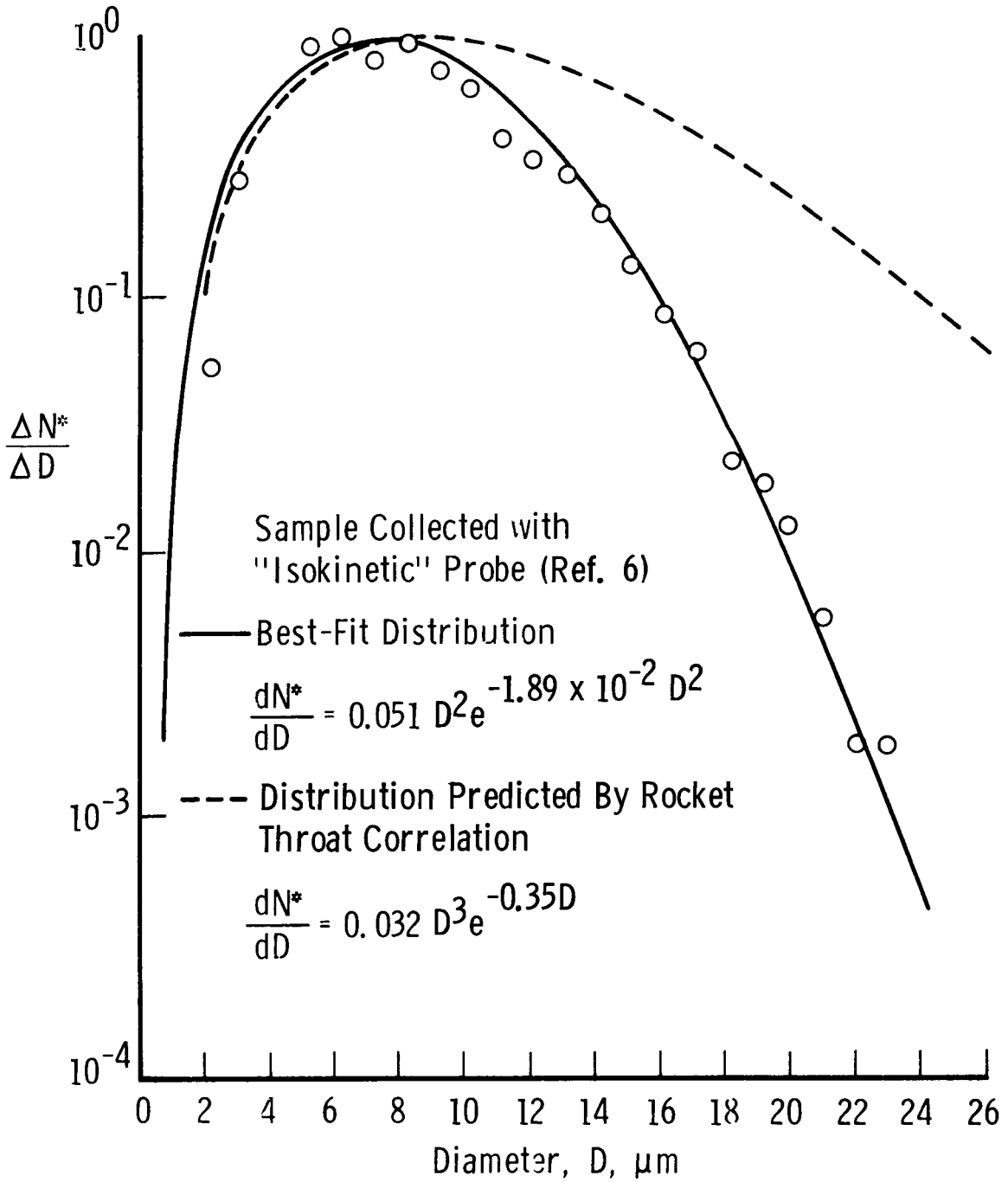

Fig. 4 Size Distribution from Titan IIIc (37.7-in Throat)

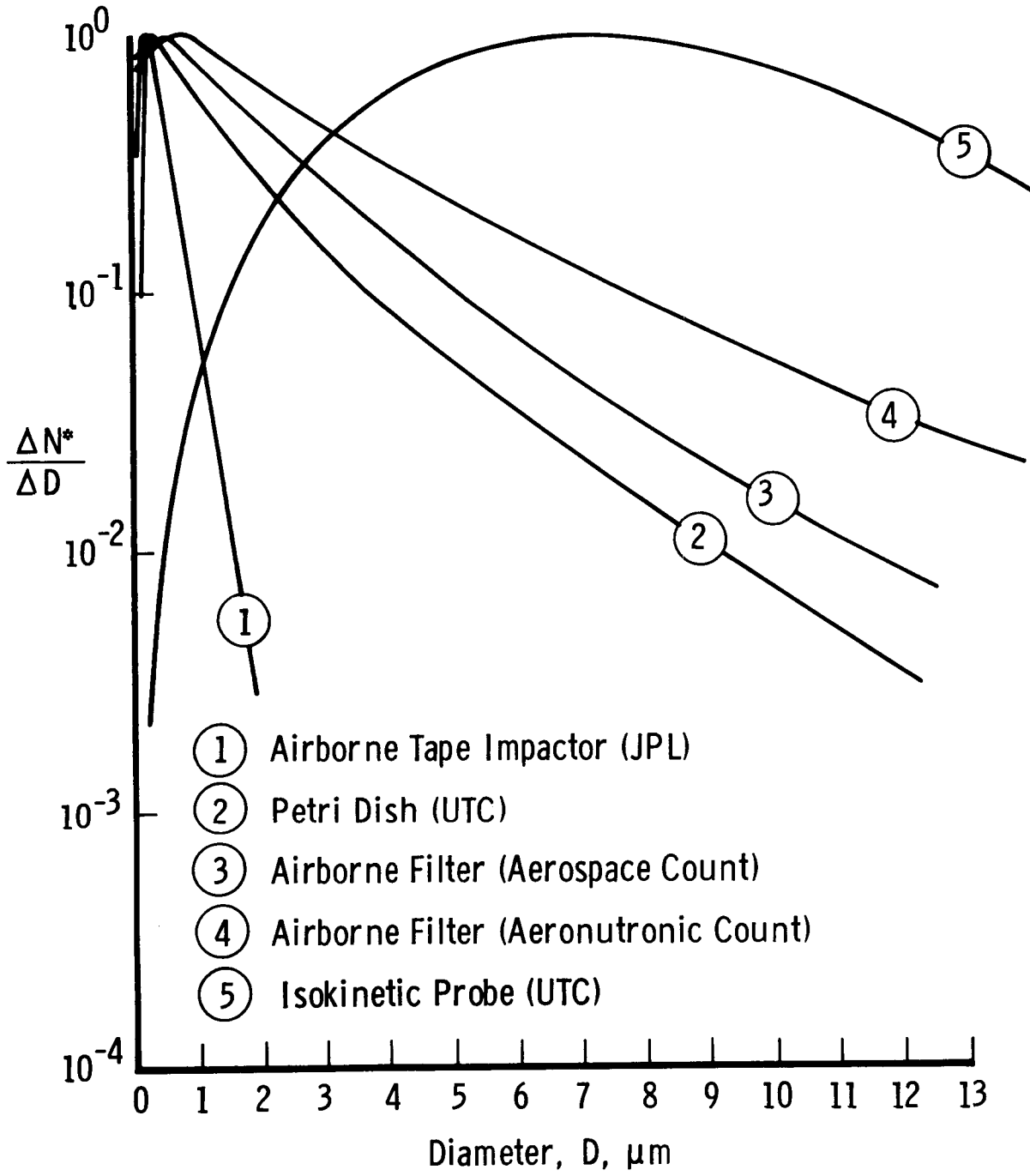

Fig. 5 Comparison of Data from Various Titan Plumes

reproducible. However, when one examines the results where the same samples were analyzed using different techniques one finds significant differences. Figures 6 and 7 present the particle size distribution curves for samples from two experimental motors with 2-in.-diam throats and different fuel mix. One method of analysis was an optical microscope and the other a scanning electron microscope (SEM). There are two points of interest in these curves. First, it is noted that there is a distinct shift to smaller particles when using the SEM. Second, this same shift occurs for each of the fuel formulations. It is possibly a trivial point, but these data emphasize the fact that even if the submicron particles are collected they cannot be counted if they cannot be seen. The SEM easily resolves particles well below the visibility of the optical microscope and thus shifts the observed size distribution. These data also serve as a reminder, that regardless of biases introduced by the particle sizing and counting technique, there is a difference due to the propellant mix.

Of particular interest are the distributions presented in Fig. 8. The samples were taken from the two extremes of rocket motors, a Titan III-C, and a small experimental motor. However, the collection technique of settled sample in Petri dishes was the same. The similarity of these data would confirm the suggestion that available data to date are more characteristic of the collection technique than the rocket motor which produced the particles. Brown et al.[5] present Al_2O_3 particle size data taken from an experimental test motor in which they were able to vary the fuel formulation (percentage of Al and size of Al powder), combustion chamber pressure, combustion chamber size and expansion ratio. They suggest that none of these parameters had significant influence on the particle size distribution which they observed (Fig. 9). However, one

---

[5]Brown, B., McArty, K. P., "Particle Size of Oxides from Combustion of Metalized Solid Propellants," 8th International Symposium on Combustion, C.I.T., Pasadena, CA, Aug.-Sept. 1960.

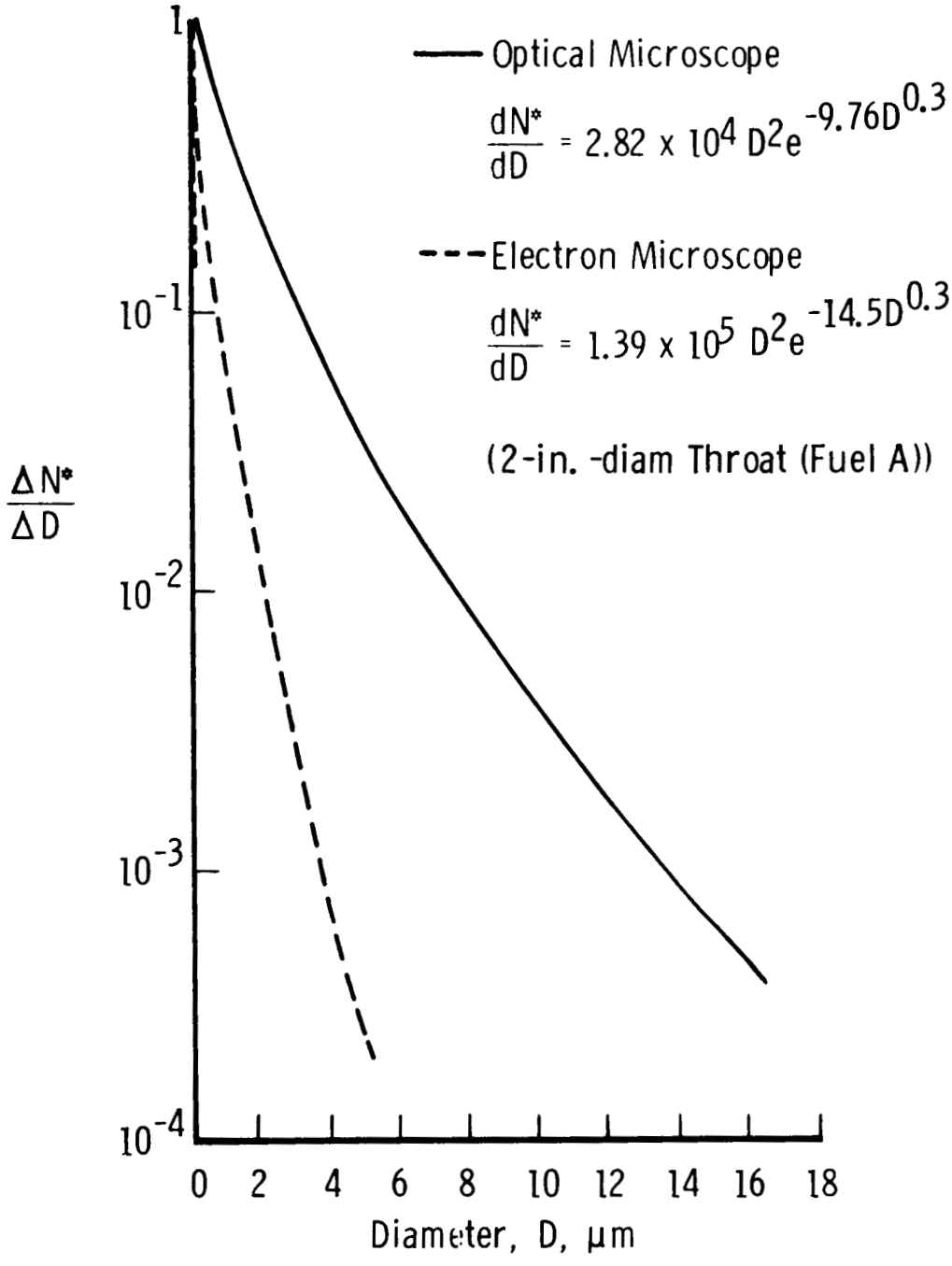

Fig. 6 Small Experimental Motor

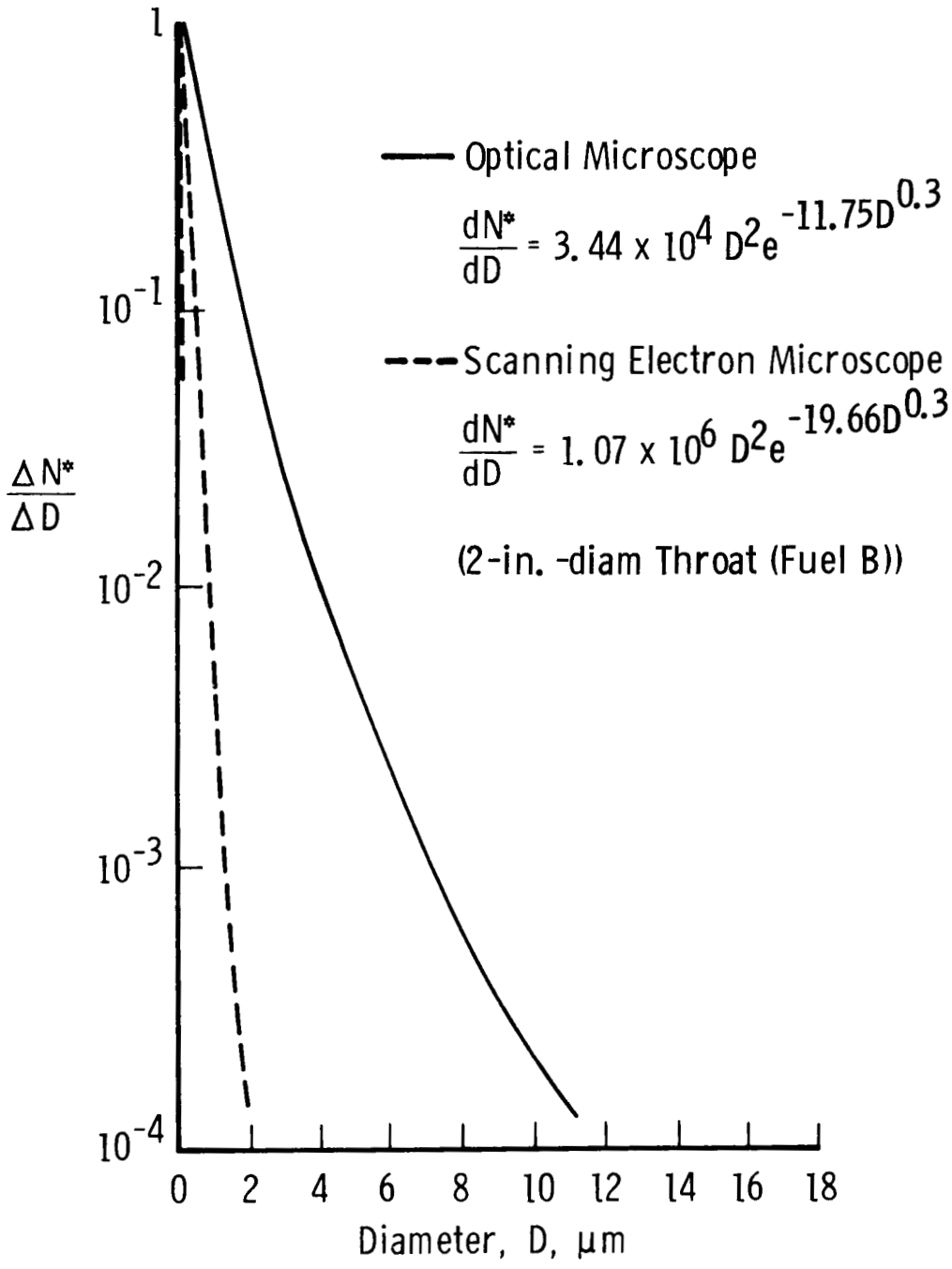

Fig. 7 Small Experimental Motor

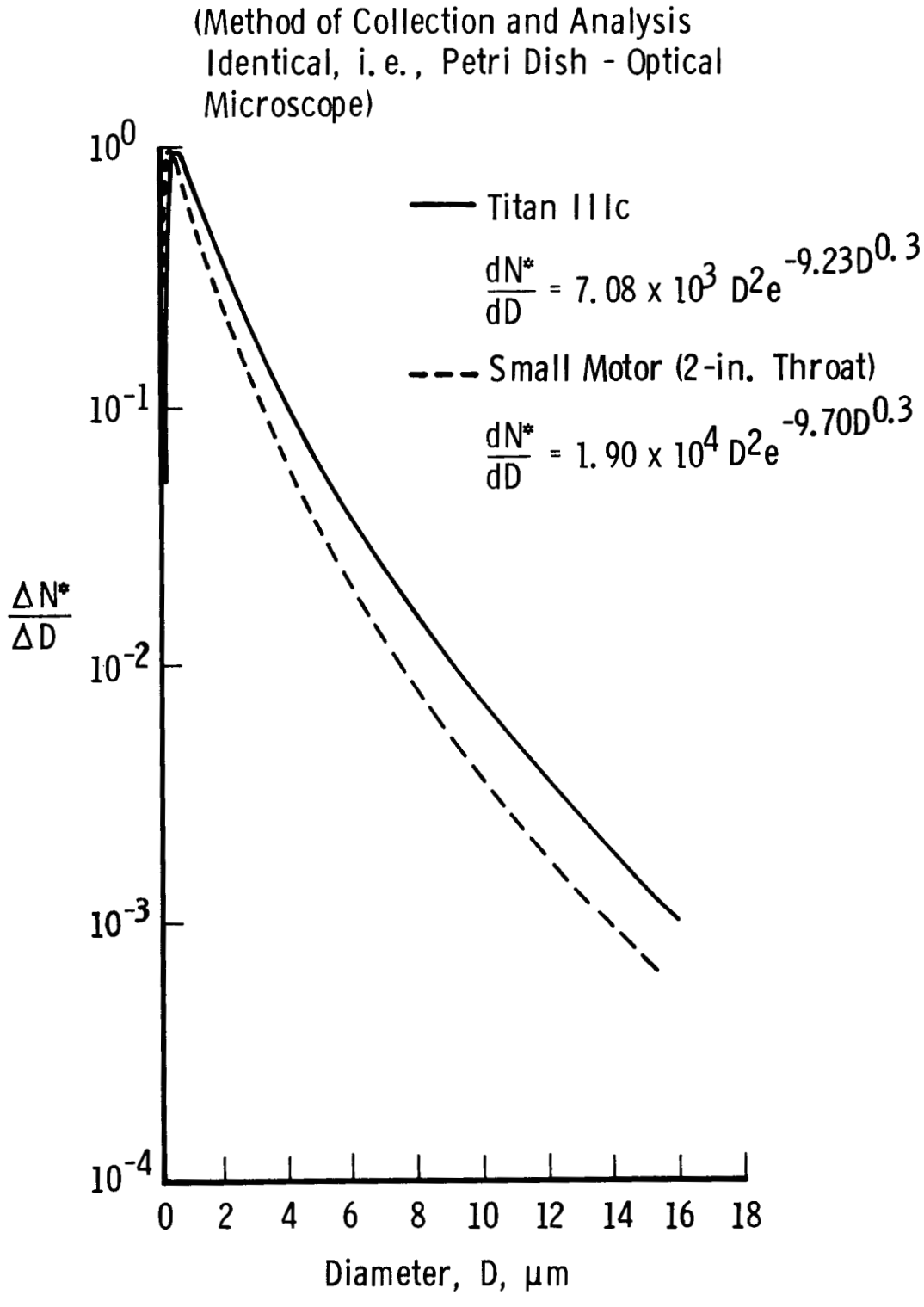

Fig. 8 Comparison of Titan and Small Motor

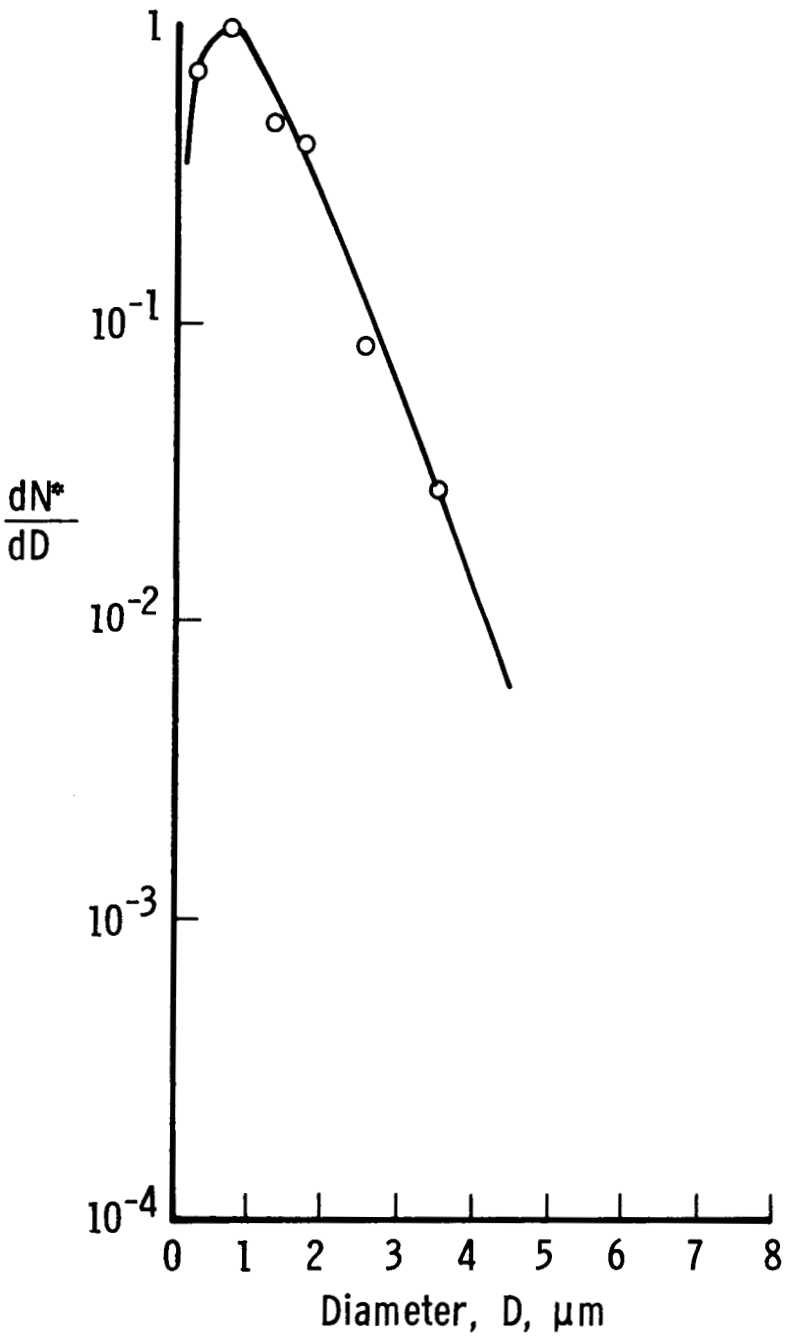

Fig. 9 Particles Collected on Impact Plates Exposed to the Exhaust Plume (Sized and Counted from SEM Photographs)

wonders if the collection technique which remained the same for all tests could possibly mask any subtle changes in the particle size distribution.

3.0 ALUMINUM OXIDE SAMPLING TECHNIQUES

The data presented thus far are representative of sampling techniques where the Al_2O_3 has been collected at a considerable distance from the rocket. Due to the obvious hostile environment close to the exhaust nozzle there are limits on where samples can be taken. A successful attempt to obtain Al_2O_3 particles on the launch platform of a Titan III-C was made by Willoughby[6] using an "isokinetic probe." This probe was aligned with the flowfield and was so constructed that the exhaust gases flowing around the probe produced a low pressure region at the base of the probe, thus drawing a sample of the rocket plume through the sampling section. Here the gases were allowed to decelerate and deposit the particles on a sampling surface.

Sampling methods may be classed as passive and active. The passive collectors include petrie dishes, polyethylene sheets, sticky tapes and even, in one case, rainwater accumulated on the roof of an automobile. The active collectors, consisting of filters and impactors (wire, flat disc, cascade, tape) where cloud samples are drawn through the collector, have been used at stationary ground points and also aboard aircraft flown through exhaust plumes.

Samples have been processed by a variety of methods to produce particle size distribution data. Where the collection technique has produced a reasonably dispersed monolayer of particles, the usual analysis has been by counting and sizing under an optical or scanning electron

---

[6] Willoughby, P. G., "Sampling and Size Determination of Particulates from the Titan III-C Exhaust Plume," United Technology, TR-33-74-U1, Feb. 1974.

microscope. In those instances where the sample was too dispersed (collected on large polyethylene sheets) or too closely packed, the sample was washed from the collector and then redistributed on an appropriate microscope slide. Usually this process involved using ultrasonic baths to try to avoid coagulation of the particles as the liquid carrier evaporated. Samples collected on filter papers have been analyzed in terms of mass loading by simply weighting the filter and also by ashing the filter and recovering the Al_2O_3 by repeated washing of the residue. An extreme pre-processing procedure is described as follows:

> "The ground sampling panels were cut into 3"-wide strips and scrubbed in 600 cc of water. The solids were filtered and the filter dried and ashed at 600°C in a porcelain crucible. The residue was treated with aqua regia and heated to just under boiling for 1/2 hour. The resulting material was cooled, diluted with water and filtered. The filter was dried and ashed at 600°C in a platinum crucible and the remaining material treated with 50 percent HF for 1/2 hour at a temperature just under boiling, the resulting material was filtered and ashed in a porcelain crucible. The Al_2O_3 particles were then sized and counted."

It can be quite easily seen from these comments on the techniques used to collect and analyze samples that there are several biases against the submicron particles.

Those samplers at ground level collecting the fallout from the exhaust, have an extremely effective atmospheric filter to remove the submicron particles. The "isokinetic probe" which removes this filter suffers from the fact that its sampling surface is an impaction collector and at the lower velocities in the probe the larger particles impact and the submicron particles flow around the surface. Devices flown through the exhaust cloud with some attempt to sample isokinetically would be

expected to produce a more representative sample. Unfortunately, in most cases what is gained in the sampling is lost in the processing, since the filters and sticky tapes employed are either burned and/or washed to extract the sample from the collector.

4.0 RESULTS FROM THE MARSHALL SPACE FLIGHT CENTER (MSFC) SAMPLING TESTS

These tests consisted of a 6.4% scaled model of the space shuttle with two Tomahawk solid rocket motors used to simulate the solid strap on boosters. The model was mounted above a scaled version of the proposed shuttle launch pad and both the solid and the liquid engines were fired simultaneously. The basic test series was conducted to evaluate the acoustic coupling between the vehicle and the launch pad at lift off. The particle collection experiments were conducted as a peripheral test to evaluate some of the techniques used in previous field tests. The particle size distributions obtained from the MSFC scaled shuttle tests are presented in Figs. 10 and 11. As can be seen in Fig. 10, the various collection techniques do bias the size distribution. It is interesting to note that the "isokinetic" probe data from these tests are quite similar to those for the UTC Titan samples.[6] The distributions presented in Fig. 11 compare the particles from the Tomahawk to other rocket motors where the sample has been collected by fallout into Petrie dishes.

4.1 Titan III-D Plume Sampling (ETR 5-20-75)

These particular data have been singled out for emphasis, in that they would appear to be the least biased by sampling and counting techniques. The data were taken by JPL under the direction of Dr. Varsi.[7] The rocket plume was produced by a Titan III-D and was sampled at an altitude of 20 km approximately 10 minutes after launch. The sampling

---

[7] Varsi, G., "Proceedings of the NASA Atmospheric Effects Working Group Meeting," Vandenburg AFB, Oct. 27-28, 1976.

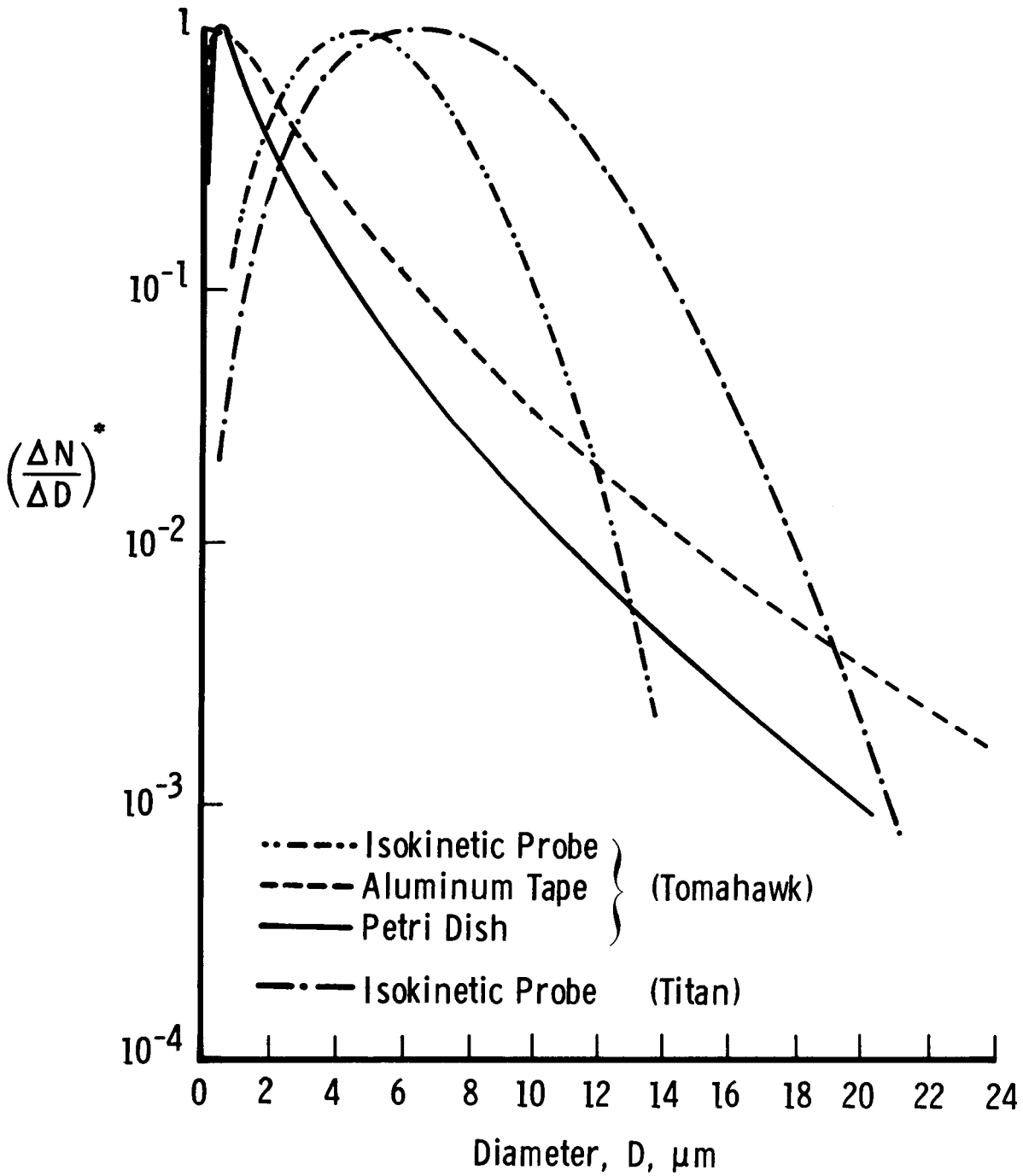

Fig. 10 Particle-Size Distributions (Tomahawk MSFC)

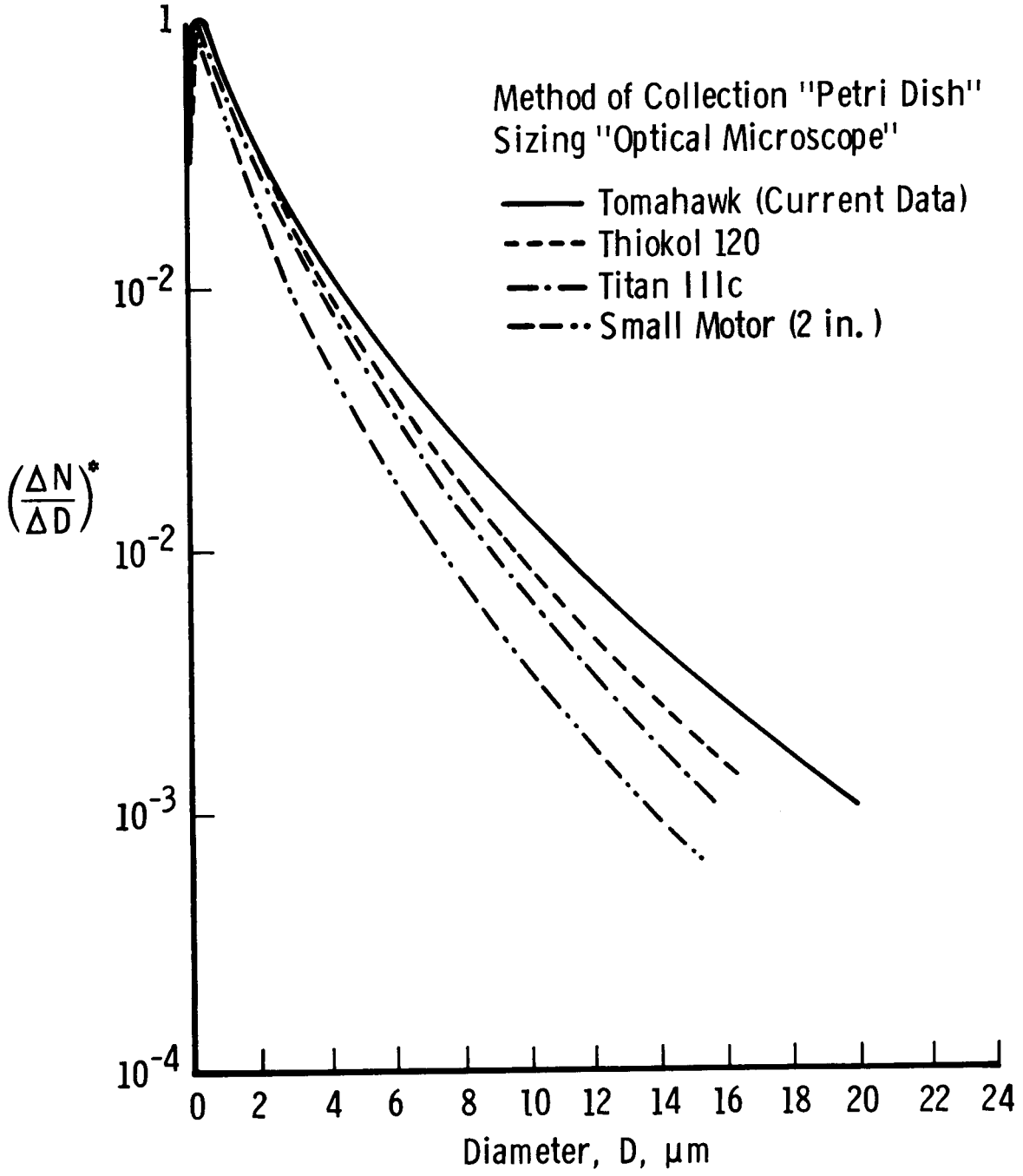

Fig. 11 Al_2O_3 Particle-Size Distributions for a Variety of Motors

aircraft flew through the plume and collected the Al_2O_3 isokinetically. Submicron sized particles were analyzed using an electric mobility analyzer and micron sized particles were collected on a moving tape impactor. An additional measurement of the total particle concentration was made using a condensation nuclei counter.

4.1.1 Electric Mobility Analyzer

The electric mobility analyzer sizes particles by drawing a sample of the aerosol through an ionization section where the particles are charged. The sample stream is then surrounded with a sheath of clean air and the flow passes between two electrodes. A known high voltage is impressed between these electrodes thus applying an attractive sideways force on the particles. If each particle has the same charge then for a particular voltage only particles of a specific size or smaller will be able to migrate through the clean air sheath to the attracting electrode. Thus by programming the high voltage applied and measuring the current flow which results from particles migrating to the electrode, a size distribution of the particles in the sample can be calculated. The instrument has a reported capability of sizing particles from .005 μm to 1.0 μm.[8] For particles larger than 1.0 μm, wall losses and ambiguities caused by multiple charging of the particles render the data questionable. Indeed the multiple charging problem can render the data questionable when the particle species are unknown since a mixture of particles can have a variety of charging properties (i.e., oil droplets, soot, clays, acid aerosols, etc.). The particle sample obtained with the mobility analyzer can be used to provide an absolute particle concentration in that the device operates with known flow rates and thus yields particle counts per volume of sampled air.

---

[8]Liu, B. Y., Fine Particles Aerosol Generation, Measurement Sampling and Analysis Academic Press, Inc., New York, 1976.

4.1.2 Tape Impactor

The tape impactor collects particles on the sticky surface of a tape which is slowly moving past the sampling orifice. The particle laden air is drawn into the sampler and accelerated through a nozzle which faces the tape. Because of their momentum, large particles (>1.0 μm) impact on the surface and are captured. Some of the smaller particles can follow the airstream as it turns and flows aroung the tape and thus there is a gradual decrease in the collection efficiency for smaller particles. Correction factors are applied to the data to account for these losses. Since the tape is constantly moving it produces a well spaced collection of particles which can later be sized and counted. The size distribution measured by the tape impactor can, however, be distorted by loss of larger particles in the inlet and nozzle section and in addition it does require extreme care in the sizing and counting since the particles are not randomly distributed on the tape surface (i.e., due to shape of nozzle and direction of tape travel the particles will tend to distribute themselves according to size).

4.1.3 Aiken Nuclei Counter

An Aiken nuclei counter does not yield a size distribution, but can give an approximate value for the number density of particles. It operates by drawing a known volume of the air into a chamber saturated with water vapor. A piston or diaphragm is then released which results in an adiabatic expansion of the vapor mixture. In this supersaturated environment water vapor condenses on all the particles present and the resulting cloud of droplets is detected by an optical sensor. The optical measurement is a simple extinction measurement and is successfully converted to a number density because of two factors. First, the water droplets observed are much larger than the original particles and therefore the unknown indices of refraction of these particles are not important. Secondly, the growth process of the water drops is such that the smaller drop radius will increase at a much faster rate than the larger

ones. Thus, the final cloud of droplets will all be close to the same size at the time of the extinction measurements. The instrument can therefore be calibrated with a known aerosol number density and be expected to hold this calibration for an unknown aerosol where the particle composition and size may be quite different.

4.1.4 Data Fitted to a Distribution Function

The particle counts per size interval from the mobility data were fitted to a distribution function as previously described. The curve was normalized to the mode and is presented in Fig. 12. The data from the tape impactor provides a second particle size distribution which partially overlaps the mobility data. However, the overlap is in a regime where the tape impactor data has large correction factors applied to allow for small particle losses. Thus a distribution function was fitted to the tape impactor data for particle sizes greater than 0.5 μm. Both sets of data indicate an inflection point around the 0.35 μm particle size and the tape impactor data was therefore scaled to match the mobility distribution at this point.

The resulting distribution is shown in Fig. 12 with data points from both instruments. The poor fit of the 0.1 μm data from the tape impactor can be accepted since in this range the instrument count has been corrected by a large and somewhat questionable loss factor. It is immediately obvious that this distribution is quite different from those presented previously. The most striking point is that its mode is in the submicron range. Since there is a delay between plume formation and sampling (T_o + 10 minutes), then the first impulse is to suspect that the larger particles have settled out. However, calculating the settling rate of a 10 μm Al_2O_3 particle and considering the 10 minute interval the total distance fallen would be approximately 9 meters. It would thus seem that this settling would be insignificant insofar as skewing the size distribution, at least up to the 10 μm particle sizes. Similar

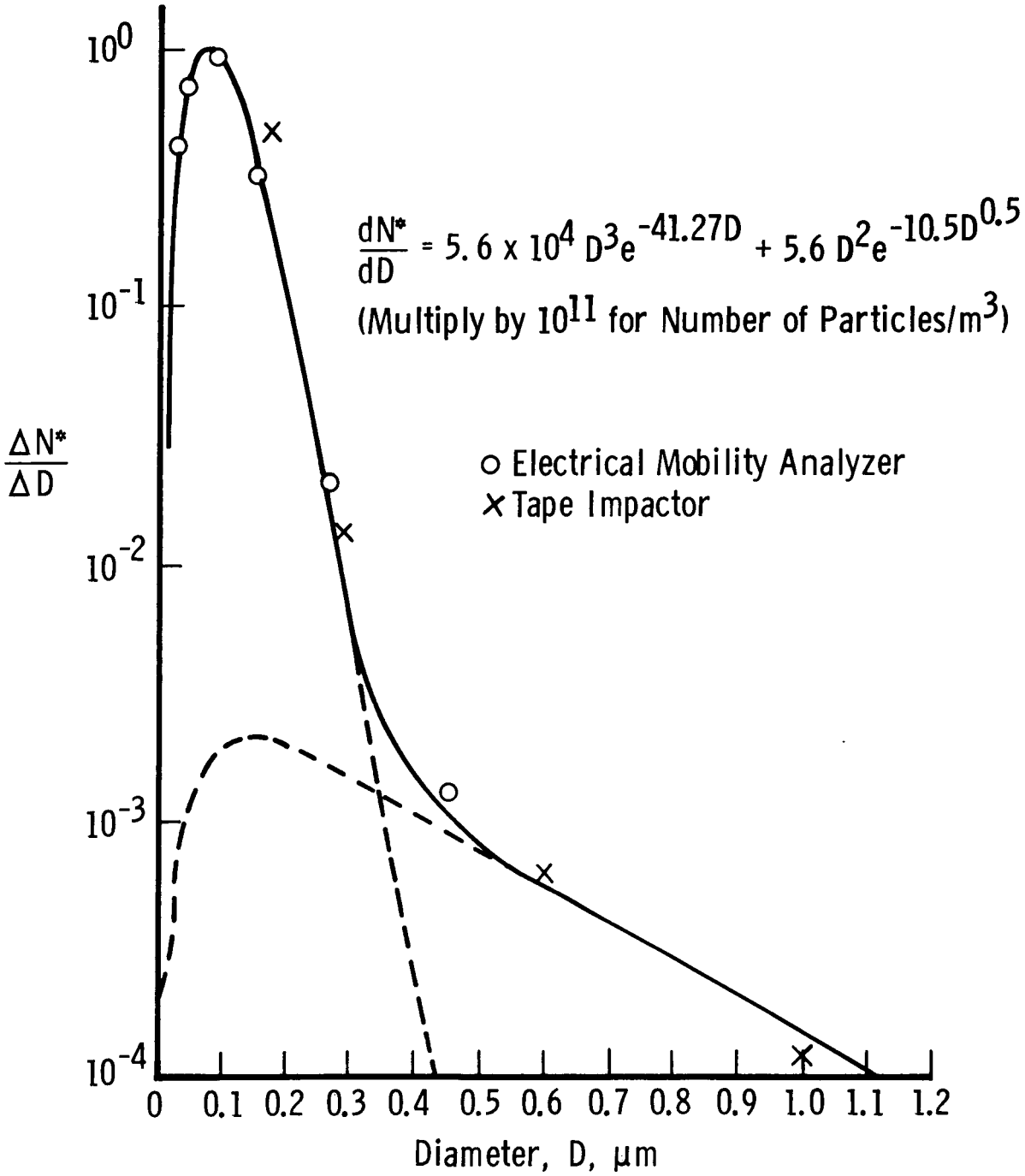

Fig. 12 Titan IIID Data Reported by Dr. Varsi (Ref. 7)

calculations for 100 μm particles suggest that they could be depleted due to gravitational settling.

The closure condition based on calculated emissions from the solid motors at 20 km altitude of 930 gms of Al_2O_3 per meter altitude and an estimated plume diameter of 2 km yields an average mass loading in the atmosphere of 2.9×10^{-4} gms/m^3.

Using the particle size distribution in Fig. 12 and adjusting the particle number density to match the value measured by the Aiken nuclei counter (i.e., 3×10^{10} particles/m^3), then the equations can be integrated to yield an atmospheric mass loading. These calculations indicate values of 5.24×10^{-5} gms/m^3 for particles sized from .025 to .525 μm and 4.78×10^{-5} gms/m^3 for particles from .525 to 6.0 μm or a total of 1.0×10^{-4} gms/m^3.

Considering the possible uncertainties of such values as the plume diameter, and the aluminum oxide deposition rate as well as the possible biases which might be included in the particle measurement techniques these values are in remarkably good agreement.

A second point of interest in these data is that the size distribution is bimodal. Kraeutle et al.[9] have observed this bimodal nature of the Al_2O_3 particle distribution in samples taken from smaller rocket motors. A size distribution from their data is shown in Fig. 13. When compared to the Titan III data it is noted that the distribution of the small particles is similar, however, the larger particles (>1 μm) are an order of magnitude more numerous. Using this distribution function and assuming a number density of 3×10^{10} particles/m^3 for the Titan plume one calculates a mass loading of 2.3×10^{-2} gms/m^3 with 10 percent of the mass in the submicron sized particles.

---

[9] Victor, A. C., Breil, S. H., "A Simple Method for Predicting Rocket Exhaust Smoke Visibility," Journal of Spacecraft and Rockets, August 1977.

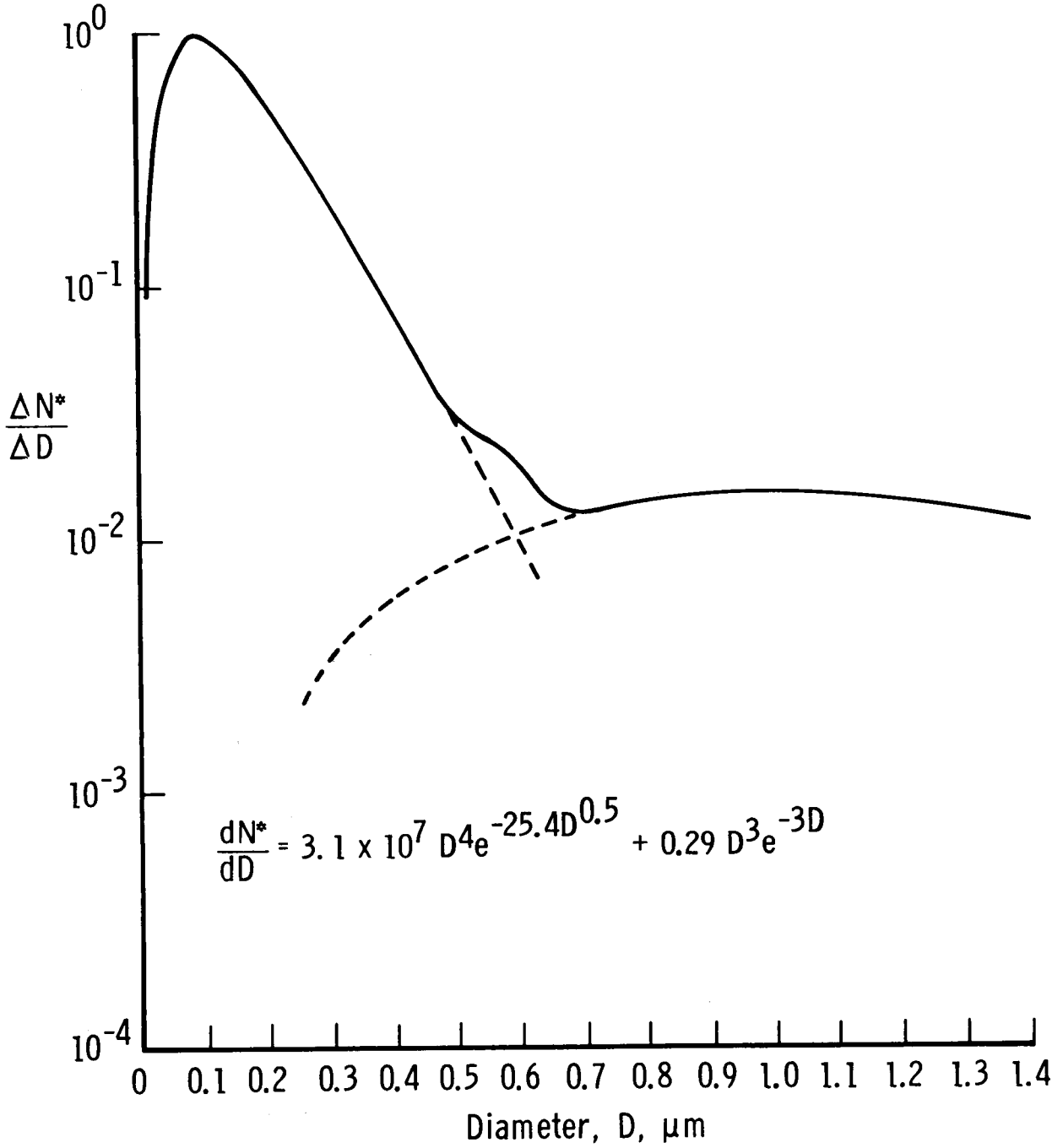

Fig. 13 Distribution Obtained by Kraeutle (Ref. 9)

Repeating this exercise with the distribution function derived from data collected by Petrie dish technique (curve 2, Fig. 5) yields a mass loading of 1.1 gms/m^3, obviously, a value orders of magnitude too high. The Kraeutle distribution is seemingly high but certainly within reason. It is unfortunate that the relatively easily obtained measurement of total particulate mass loading was not made on the Titan cloud fly-through. This information would be of great value in evaluating the validity of various distribution functions.

5.0 ALUMINUM COMBUSTION

The problem of aluminum combustion and its oxide formation has received a great deal of attention and has been extensively reported in the literature. However, due to the extremely hostile environment in the combustion chamber and nozzle expansions of the exhaust gases from solid rocket motors the physical and chemical processes occurring which results in the eventual aluminum oxide particles observed downstream, are not well known. A good review of the many facets of the problem is presented by Pokhil et al.[10] More specific studies of the problems associated with aluminum combustion both in the rocket environment and under controlled laboratory conditions are presented in work such as that by Crump et al.[11] and Prentice.[12] From these and similar studies the following observations can be made.

---

[10]Pokhil, P. F., Belyayev, A. F., Frolov, Yu, V., Logachev, V. S., and Korotkov., A. I., "Combustion of Powdered Metals in Active Media," FTD-MT-24-551-73, 1972.

[11]Crump, J. E., Prentice, J. L. and Kraeutle, K. J., "Role of the Scanning Electron Microscope in the Study of Solid Propellant Combustion: II Behavior of Metal Additives," Combustion Science & Technology, 1969, Vol. 1, pp. 205-223.

[12]Prentice, J. L., "Aluminum Droplet Combustion Rates and Mechanisms in Wet and Dry Oxidizers," NWC-TP-5569, April 1974.

1. The molten aluminum droplets in the combustion chamber are, in general, considerably larger than the particles of aluminum included in the fuel. It is noted that as the fuel surface recedes, the aluminum particles are exposed and tend to cluster. Rather than leave the surface immediately they melt and form a liquid Al and solid Al_2O_3 matrix before being swept into the gas stream. This process of agglomeration thus suggests that the final Al_2O_3 particle size cannot be directly related to the original size of metallic aluminum particles in the fuel. The degree of agglomeration is influenced by several factors which include, initial particle sizes of both fuel and oxidizer, uniformity of mixture, type of binder, rate of burning, pressure in combustion chamber and thickness of oxide coating on the metallic aluminum particles used in the fuel.[13]

2. During the melting and agglomeration process, the oxide coatings from the original aluminum particles crack open and accumulate on the surface of the droplets. As the heating process continues these shell fragments melt and form a visible lens cap like structure on the surface of the spherical molten aluminum.

3. Ignition appears to occur as the molten Al-Al_2O_3 droplet leaves the surface and enters the high temperature combustion zone. From high speed photographs it is observed that the flame stands off from the surface of the droplet thus indicating a gas phase reaction. Due to the continuum radiation produced from all the Al_2O_3 in the combustion chamber it is impossible to distinguish any spectra indicating the occurrence of the suboxides AlO and Al_2O. However, supplementing evidence from the ignition of aluminum filled flash bulbs does show emission lines of AlO.[10,14]

---

[13]Crump, J. E. (Editor), "Combustion of Solid Propellants and Low Frequency Combustion Instability," NOTS-TP-4244, June 1967.

[14]Herzberg, G., Molecular Spectra and Molecular Structure, Spectra of Diatomic Molecules, D Van Nostrand Co., Inc., New York, New York, 1950.

Porter et al.[15] studied the species vaporizing from an Al-Al_2O_3 mixture using a mass spectrometer. Their system was limited to temperatures of 1800°K, however, they identified Al and Al_2O as the prime gaseous constituents with a trace signal of AlO. Brewer et al.[16] conducted similar vaporization experiments and concluded that in the Al-Al_2O_3 mixture the basic sub-oxide is Al_2O whereas in the vaporization of Al_2O_3 alone AlO is the dominant gas species. It was also observed that when molten aluminum was in contact with the Al_2O_3 this increased the evaporation rate of the Al_2O_3 by two orders of magnitude.

Considering these comments and then returning to the observations of molten aluminum droplets with molten lens caps of Al_2O_3 surrounded by a reactive flame zone, it can be seen that the production of aluminum oxide particles in a rocket motor is a complex process. The sub-oxides are obviously formed in the reaction zone surrounding the burning droplet, with possible additions from the evaporation of Al_2O_3 at the Al-Al_2O_3 interface on the droplet. Adding to this complexity is the fact that the droplets and gases are swept from the surface of the burning propellant and are rapidly accelerated through the nozzle and into the expanding plume. However, from these observed processes one can speculate that there are at least two possible sources of Al_2O_3 particles, the liquid Al_2O_3 lens caps which remain as residue after the Al has evaporated and Al_2O_3 formed from the condensation of the gaseous sub-oxides.

---

[15] Porter, R. F., Schissel, P., Ingram, M. G., "A Mass Spectrometric Study of Gaseous Species in the Al-Al_2O_3 System," Journal of Chem. Phys., Vol. 23, No. 2, Feb. 1955.

[16] Brewer, L. and Searcy, A. W., "The Gaseous Species of the Al-Al_2O_3 System," Journal Am. Chem. Soc., Vol. 73, 1951.

5.1 Condensation of Gaseous Oxides

There is no experimental evidence that either of the sub-oxides can exist in the solid or liquid phase. Material identified by Hoch et al.[17] as solid Al_2O and AlO was later shown to be Al_4C_3 and $AlTaO_4$ by Yanagida.[18] Thus the condensation of gaseous AlO-Al_2O to Al_2O_3 is both a chemical and physical process. Hermsen[19] has applied the classical homogeneous nucleation theory as presented by Frenkle[20] to predict nucleation rates. To circumvent the problem of not being able to define a supersaturation of the AlO-Al_2O gas, he uses the ratio of the partial pressure of the Al gas to the equilibrium vapor pressure of Al gas in Al_2O_3 vaporization products. Regardless of the confidence one might have in this treatment of the problem, the predicted nucleation rates are of questionable value since they vary by a factor of 10^{16} over the temperature range of interest (i.e., 3000°K to 3500°K). It would thus seem that until the condensation process can be identified, it is premature to try to adapt existing condensation theories to predict nucleation rates. While the actual process involved in the condensation of the sub-oxides is not yet known it is not unreasonable to suggest that condensation is the source of the submicron particles observed in the rocket exhaust plume.

---

[17] Hoch, M. and Johnston, H. L. "Formation Stability and Crystal Structure of the Solid Aluminum Sub-oxides: Al_2O and AlO," Journ. Am. Ceramic Soc., Vol. 76, 1954.

[18] Yanagida, H., Kroger, F. A., "Condensed Phases in the System Al_2O_3-Al," Ceramic Bulletin, Vol. 23, 1955.

[19] Hermsen, R. W., Dunlap, R., "Nucleation and Growth of Oxide Particles in Metal Vapor Flames," Combustion & Flame, Vol. 13, No. 3, June 1969.

[20] Frenkle, J. Kinetic Theory of Liquids, Oxford University Press, London, 1946, p. 397.

5.2 Dispersion of Liquid Al_2O_3

It has been noted that due to an agglomeration process at the burning surface of the fuel, relatively large droplets of molten aluminum with attached Al_2O_3 lens caps, enter the gas flowfield. A typical histogram of these agglomerated droplet sizes as measured by Boggs et al.[14] is reconstructed in Fig. 14. From the scaled photographs of burning droplets as shown in Ref. 13, one can estimate that the volume of liquid Al_2O_3 in the lens cap is approximately 0.8 percent that of the molten aluminum droplet. The order of magnitude of this value is confirmed by the observation that the original aluminum powder (approx. 15 μm diam) has on the average a 75-Å-thick coating of Al_2O_3.[21] Assuming negligible evaporation or condensation of the liquid Al_2O_3 then one can predict a range of residual alumina droplets from 4 to 40 μm in diameter based on the agglomerated particle sizes shown in Fig. 14.

It is also observed that a considerable quantity of liquid Al_2O_3 accumulates on the nozzle walls and is shed due to the high velocity gases. Bartlett et al.[22] have used the droplet stability criteria of a critical Bond number to calculate the maximum size of a molten aluminum oxide droplet which could survive the aerodynamic forces in the rocket flowfield. In a similar manner one can postulate the maximum aerodynamic drag forces which might be encountered and equating these forces to the surface tension of liquid Al_2O_3[23] calculate that the minimum droplet size produced by this mechanism is on the order of 1 μm. It would thus appear that the agglomeration process at the burning surface and

---

[21] Price, E. W., "Summary Report on Workshop on Behavior of Aluminum in Solid Propellant Combustion," Proceedings of the 13th JANNAF Combustion Meeting, Nov. 1976.

[22] Bartlett, R. W., Delaney, L. J., "Effect of Liquid Surface Tension on Maximum Particle Size in Two Phase Flow," Pyrodynamics, Vol. 4, 1966.

[23] Kingery, W. D., "Surface Tension of Some Liquid Oxides and Their Temperature Coefficients," Journal of the American Ceramic Society, Vol. 42, No. 1, Jan. 1959.

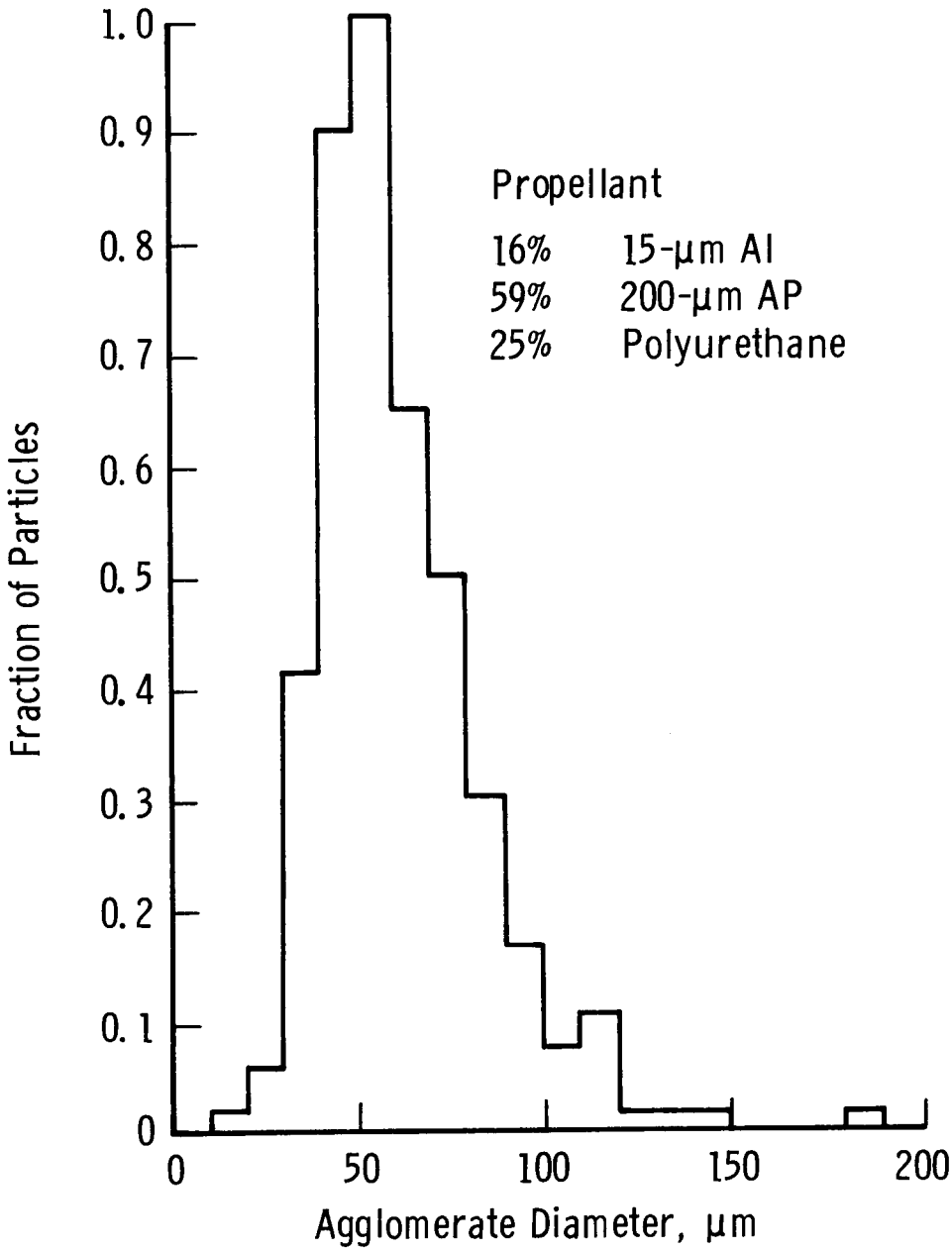

Fig. 14 Agglomerate Diameters in Aluminized Propellant (Ref. 14)

aerodynamic dispersal of liquid Al_2O_3 provide particles in the micron size range.

6.0 CONCLUSIONS

From the observations cited, there is ample evidence to support a multimodal distribution function for the Al_2O_3 particle sizes. If as has been suggested the larger particles are produced by an agglomeration and dispersal process and the smaller ones by condensation then an argument can be made in favor of the strong submicron particles mode of the Varsi distribution. In the large motors such as Titan, Super Hippo and Shuttle the agglomerated droplets are confined in the combustion zone ($\sim 3500^{o}K$) for a much longer period than in small motors. In this environment the liquid Al_2O_3 droplets from the agglomeration process are in a reducing atmosphere of Al gas and thus are evaporating. If this evaporation yields Al_2O, then it is not rate controlled by the partial pressure of AlO produced by the combustion of the aluminum directly in the oxidizer. The net result would be a depletion in the number and size of liquid Al_2O_3 droplets and an increase in the sub-oxides which would participate in a chemico-physical condensation process. This argument does not consider the additional processes of particle growth, coagulation and remelting which might occur in the exhaust flowfield. It does, however, question the accepted viewpoint that bigger motors produce bigger particles, and, in fact, suggests that the reverse may be true. That is, the larger motors may be more efficient in reducing the Al_2O_3 contained in the initial fuel and thus primarily produce Al_2O_3 particles through condensation processes.

These factors plus the noted bias in previous data thus argue in favor of the bimodal particle size distribution functions as derived from data by Varsi and Kraeutle with significant quantities of Al_2O_3 contained in the submicron particles.

It is unfortunate, but notwithstanding all the previous efforts to determine the particle size distribution of Al_2O_3 in rocket plumes, it appears that further measurements, preferably made within the exhaust cloud, are still needed. In order that the data can be checked for consistency, three types of measurements should be made. The first and possibly the easiest measurement is total mass loading in the cloud. This measurement can be made using absolute filters for average values or possibly QCM's in conjunction with a precipitator (electrostatic or inertial) for determining cloud profiles. The second measurement needed is a count of the total number of particles per unit volume. A condensation nuclei counter could yield this data. The third measurement is the particle size distribution. No one instrument can cover the size range of interest (.005 to 50 μm). The electric mobility analyzer would appear to be the most promising for the .005 to .5 μm size range. Inertial impactors can operate effectively over a range from .1 μm to 10 μm. A cascade impactor with QCM readout at each stage could give near real time readout and thus indicate the homogeneity of the cloud section sampled. The particles ranging from .5 μm to 50 μm can be detected by optical scattering and there is a variety of instruments available.

It should be noted that all of these measurements including the simple total mass determined from weighing collections on filters, will be compromised if there are significant numbers of condensed water or acid droplets in the cloud. This requires that the rocket cloud therefore be formed in a relatively dry atmosphere and thus adds an additional constraint to the problem of cloud sampling.

Additional studies of the basic mechanisms of Al_2O_3 particle formation would be worthwhile, since if the condensation and coagulation process is occurring to a significant extent outside the combustion chamber and nozzle, then the Al_2O_3 particles deposited in the stratosphere and space can be quite different from those observed at low altitude due to the significant differences in the plume expansion. This would especially

be of concern in the operation of the solid rocket motor for the interim upper stage (IUS) of the space shuttle operations.

ACKNOWLEDGMENT

The work reported herein was sponsored by NASA Marshall Space Flight Center, and performed by the Arnold Engineering Development Center (AEDC), Air Force Systems Command (AFSC). Work and analysis were done by personnel of ARO, Inc., A Sverdrup Corporation Company, operating contractor of AEDC.

REFERENCES

1. Dehority, G. L., "A Parametric Study of Particulate Damping Based on the Model of Temkin andDobbins," NWC TP 5002 (Sept. 1970).
2. Nukijama, S. and Tanassawa, Y., "An Experiment on the Atomization of Liquid by Means of an Air Stream (1st report)," Trans. S.M.E. Japan, Vol. 4, No. 14 (Feb. 1938).
3. Worster, B. W. and Kadamiya, R. H., "Rocket Exhaust Aluminum Oxide Particle Properties," ARl RR-30 (Aug. 1973).
4. Rosin, P. and Rammler, E., "The Laws Governing the Fineness of Powdered Coal," Journal of the Inst. of Fuel, Vol. 7 (1933).
5. Brown, B., McArty, K. P., "Particle Size of Oxides from Combustion of Metalized Solid Propellants," 8th International Symposium on Combustion, C.I.T., Pasadena, California (Aug.-Sept. 1960).
6. Willoughby, P. G., "Sampling and Size Determination of Particulates from the Titan III-C Exhaust Plume," United Technology, TR-33-74-U1 (Feb. 1974).
7. Varsi, G., "Proceedings of the NASA Atmospheric Effects Working Group Meeting," Vandenburg AFB (Oct. 27-28, 1976).
8. Liu, B. Y., Fine Particles Aerosol Generation, Measurement Sampling and Analysis, Academic Press, Inc., New York (1976).

9. Victor, A. C., Breil, S. H., "A Simple Method for Predicting Rocket Exhaust Smoke Visibility," Journal of Spacecraft and Rockets (Aug. 1977).

10. Pokhil, P. F., Belyayev, A. F., Frolov, Yu, V., Logachev, V. S., and Korotkov, A. I., "Combustion of Powdered Metals in Active Media," FTD-MT-24-551-73 (1972).

11. Crump, J. E., Prentice, J. L., and Kraeutle, K. J., "Role of the Scanning Electron Microscope in the Study of Solid Propellant Combustion: II Behavior of Metal Additives," Combustion Science & Technology (1969), Vol. 1, pp. 205-223.

12. Prentice, J. L., "Aluminum Droplet Combustion Rates and Mechanisms in Wet and Dry Oxidizers," NWC-TP-5569 (April 1974).

13. Crump, J. E. (Editor), "Combustion of Solid Propellants and Low Frequency Combustion Instability," NOTS-TP-4244 (June 1967).

14. Herzberg, G., Molecular Spectra and Molecular Structure, Spectra of Diatomic Molecules, D. Van Nostrand Co., Inc., New York, N. Y. (1950).

15. Porter, R. F., Schissel, P., Ingram, M. G., "A Mass Spectrometric Study of Gaseous Species in the Al-Al_2O_3 System," Journal of Chem. Phys., Vol. 23, No. 2 (Feb. 1955).

16. Brewer, L. and Searcy, A. W., "The Gaseous Species of the Al-Al_2O_3 System," Journal Am. Chem. Soc., Vol. 73 (1951).

17. Hoch, M. and Johnston, H. L., "Formation Stability and Crystal Structure of the Solid Aluminum Sub-oxides: Al_2O and AlO," Journ. Am. Ceramic Soc., Vol. 76 (1954).

18. Yanagida, H. and Kroger, F. A., "Condensed Phases in the System Al_2O_3-Al," Ceramic Bulletin, Vol. 23 (1955).

19. Hermsen, R. W. and Dunlap, R., "Nucleation and Growth of Oxide Particles in Metal Vapor Flames," Combustion & Flame, Vol. 13, No. 3 (June 1969).

20. Frenkle, J., Kinetic Theory of Liquids, Oxford University Press, London (1946), p. 397.

21. Price, E. W., "Summary Report on Workshop on Behavior of Aluminum in Solid Propellant Combustion," Proceedings of the 13th JANNAF Combustion Meeting (Nov. 1976).

22. Bartlett, R. W. and Delaney, L. J., "Effect of Liquid Surface Tension on Maximum Particle Size in Two Phase Flow," Pyrodynamics, Vol. 4 (1966).

23. Kingery, W. D., "Surface Tension of Some Liquid Oxides and Their Temperature Coefficients," Journal of the American Ceramic Society, Vol. 42, No. 1 (January 1959).